Characterization of Globular Protein Solutions by Dynamic Light Scattering, Electrophoretic Mobility, and Viscosity Measurements

3 AUTHORS:

Barbara Jachimska
Polish Academy of Sciences
38 PUBLICATIONS **623** CITATIONS

SEE PROFILE

Monika Wasilewska
Instytut Katalizy i Fizykochemii Powierzch…
17 PUBLICATIONS **348** CITATIONS

SEE PROFILE
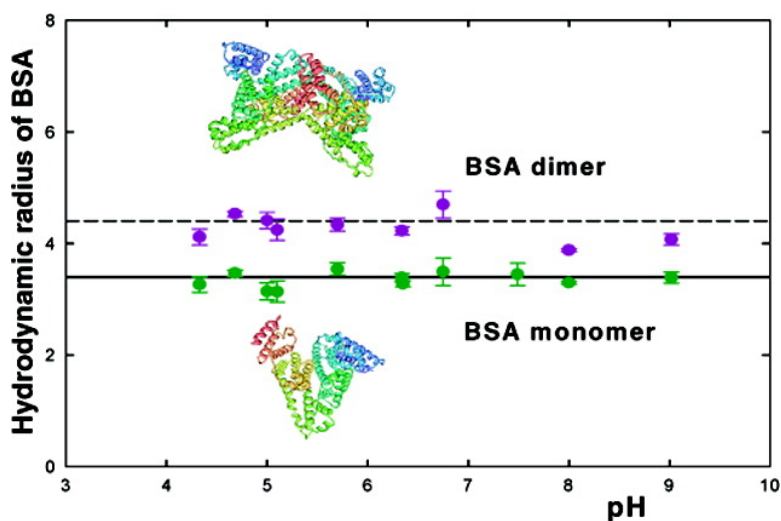
Zbigniew Adamczyk
Akademickie Centrum Komputerowe CYFR…
177 PUBLICATIONS **3,725** CITATIONS

SEE PROFILE

Characterization of Globular Protein Solutions by Dynamic Light Scattering, Electrophoretic Mobility, and Viscosity Measurements

Barbara Jachimska, Monika Wasilewska, and Zbigniew Adamczyk

More About This Article

Additional resources and features associated with this article are available within the HTML version:

- Supporting Information
- Links to the 1 articles that cite this article, as of the time of this article download
- Access to high resolution figures
- Links to articles and content related to this article
- Copyright permission to reproduce figures and/or text from this article

View the Full Text HTML

Characterization of Globular Protein Solutions by Dynamic Light Scattering, Electrophoretic Mobility, and Viscosity Measurements

Barbara Jachimska,* Monika Wasilewska, and Zbigniew Adamczyk

Institute of Catalysis and Surface Chemistry, Polish Academy of Science, ul. Niezapominajek 8, 30-239 Cracow, Poland

In this work, physicochemical properties of two globular proteins—bovine serum albumin (BSA) having a molecular weight of 67 kDa and human serum albumin (HSA) having a molecular weight of 69 kDa—were characterized. The bulk characteristics of these proteins involved the diffusion coefficient (hydrodynamic radius), electrophoretic mobility, and dynamic viscosity as a function of protein solution concentration for various pH values. The hydrodynamic radius data suggested an association of protein molecules, most probably forming compact dimers. Using the hydrodynamic diameter and the electropheretic mobility data allowed the determination of the number of uncompensated (electrokinetic) charges on protein surfaces. The electrophoretic mobility data were converted to zeta potential values, which allowed one to determine the isoelectric point (iep) of these proteins. It was found to be at pH 5.1 for both proteins, in accordance with previous experimental data and theoretical estimations derived from amino acid composition and pK values. To determine further the stability of protein solutions, dynamic viscosity measurements were carried out as a function of their bulk volume concentration for various pH values. The intrinsic viscosity derived from these measurements was interpreted in terms of the Brenner model, which is applicable to hard spheroidal particles. It was found that the experimental values of the intrinsic viscosity of these proteins were in good agreement with this model when assuming protein dimensions of $9.5 \times 5 \times 5$ nm^3 (prolate spheroid). The possibility of forming linear aggregates of association degree higher than 2 was excluded by these measurements. It was concluded that the combination of dynamic viscosity and dynamic light scattering can be exploited as a convenient tool for detecting not only the onset of protein aggregation in suspensions but also the form and composition of these aggregates.

Introduction

Protein adsorption and deposition (irreversible adsorption) on boundary surfaces is significant for a variety of disciplines including geophysics (evolution of life), material and food sciences, and the pharmaceutical and cosmetic industries. In the medical sciences, it has been determined that thrombosis formation on cardiovascular and other implants is induced by protein deposition.[1] Protein adsorption processes are also involved in blood coagulation, artificial organ failure, plaque formation, fouling of contact lenses and heat exchangers, and ultrafiltration and membrane filtration units. However, controlled protein adsorption on various surfaces is a prerequisite of their efficient separation and purification by chromatography and filtration for biosensing, bioreactors, and immunological and serological assays. Because of their fundamental and practical significance, numerous studies have been carried out over last few the decades with the aim of evaluating protein deposition kinetics and adsorption isotherms of various surfaces.[1–10]

However, the proper description and control of protein deposition phenomena require a thorough knowledge of their structural and transport properties in the bulk, primarily including their shape, conformation, degree of hydration, charge, diffusion coefficients, and aggregation degree in relation to protein bulk concentration, electrolyte composition (ionic strength), pH, and temperature. Despite rapid progress in the field of protein structural characterization,[11–13] there exist few experimental methods that can be efficiently used to determine these parameters in dilute aqueous solutions of proteins.

One class of the most rapid, noninvasive, and direct methods is represented by the hydrodynamic methods involving dynamic light scattering (DLS), dynamic viscosity, sedimentation velocity, fluorescence depolarization, and circular dichroism (CD) measurements.[14]

In this work, we applied hydrodynamic methods to characterize the dynamic properties of globular proteins in electrolyte solutions. These hydrodynamic characteristics were supplemented by the electrophoretic mobility measurements, which allowed one to determine the isoelectric point of proteins and the amount of uncompensated (electrokinetic) charge.

Materials

In our studies, essentially fatty acid and globulin-free bovine serum albumin BSA (fraction V, lyophilized powder, 99%) and human serum albumin HSA (crystallized and lyophilized powder,

* Corresponding author. E-mail: ncjachim@cyf-kr.edu.pl.

(1) Haynes, C. A.; Norde, W *Colloids Surf., B* **1994**, *2*, 517–566.
(2) Golander, C. G.; Kiss, E. *J. Colloid Interface Sci.* **1988**, *121*, 240–253.
(3) Fitzpatrick, H.; Luckham, P. F.; Eriksen, S.; Hammond, K *Colloids Surf.* **1992**, *65*, 43–49.
(4) Liebmann-Vinson, A.; Lander, L. M.; Foster, M. D.; Brittain, W. J.; Vogler, E. A.; Majkrzak, C. F.; Satija, S *Langmuir* **1996**, *12*, 2256–2262.
(5) Su, T. J.; Lu, J. R.; Thomas, R. K.; Cui, Z. F. *J. Phys. Chem. B* **1999**, *103*, 3727–3736.
(6) Rezwan, K.; Meier, L. P.; Rezwan, M.; Voros, J.; Textor, M.; Gauckler, L. J. *Langmuir* **2004**, *20*, 10055–10061.
(7) Rezwan, K.; Meier, L. P.; Gauckler, L. J .*Langmuir* **2005**, *21*, 3493–3497.
(8) Toscano, A.; Santore, M. M. *Langmuir* **2006**, *22*, 2588–2599.
(9) Kaufman, E. D.; Beleyea, J.; Johnson, M. C.; Nicholson, Z. M.; Ricks, J. L.; Shah, P. K.; Bayless, M.; Pettersson, T.; Feldoto, Z.; Blomberg, E.; Claesson, P.; Franzen, S. *Langmuir* **2007**, *23*, 6053–6062.
(10) Desroches, M.; Chaudhary, N.; Omanovic, S. *Biomacromolecules* **2007**, *8*, 2836–2844.
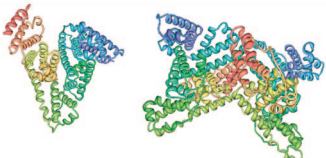
(11) Stradner, A.; Sedgwick, H.; Cardinaux, F.; Poon, W. C.; Egelhaaf, S. U.; Schurtenberger, P. *Nature* **2004**, *432*, 492–495.
(12) Stradner, A.; Cardinaux, F.; Schurtenberger, P. *J. Phys. Chem. B* **2006**, *110*, 21222–21231.
(13) Tanaka, N.; Nishizawa; H.; Kunugi; S, *Biochem. Biophys. Acta* **1997**, *1338*, 13–20.
(14) Harding, S. E. *Biophys. Chem.* **1995**, *55*, 69–93.

Table 1. Molecular Shapes and Physicochemical Properties of Proteins

Protein Property	BSA	HSA
Molecular weight [Da]	67000	69000
Specific density [g·cm⁻³]	1.35	1.35
Specific volume [nm³]	82.4	85
Equivalent sphere radius [nm]	2.70	2.72
Hydrodynamic radius R_H [nm]	3.3 − 4.3	3.3 − 4.1
Geometrical dimensions, spheroid [nm]	9.5 x 5 x 5	9.5 x 5 x 5
Geometrical volume for spheroid [nm³]	124	124
Porosity	0.33	0.33
Molecular shapes	HSA, BSA Monomer Dimer	

99%) were used. These products were purchased from Sigma and used without further purification. Physicochemical properties of the protein are given in Table 1. Tris, Mes, and Mes−Tris buffers with different NaCl concentrations ($I = 10^{-3}$, 5×10^{-3}, 10^{-2}, and 0.15 M) were used. Protein solutions of the concentrations in the range of 500−8000 ppm were used immediately after preparation. The protein concentration in solution was determined with a Shimadzu UV−vis spectrometer equipped with a quartz cell with 1 cm path length, and the absorbance was measured at 280 nm for BSA and HSA.

Doubly distilled water was used for the preparation of all solutions. Sodium chloride, HCl, and NaOH were commercial products of Aldrich and Sigma. NaCl was used as a background electrolyte. All electrolyte solutions were filtered using a 0.22 μm Millipore filter. The temperature of the experiments was kept constant at 293 ± 0.1 K (20 ± 0.1 °C).

Methods

Dynamic Light Scattering and Zeta Potential Measurements. Protein size was determined by dynamic light scattering (DLS) using the Zetasizer Nano ZS Malvern instrument (measurement range of 0.6 nm to 6 μm). The Nano ZS instrument incorporates noninvasive backscattering (NIBS) optics. This technique measures the time-dependent fluctuations in the intensity of scattered light that occur because particles undergo Brownian motion. The analysis of these intensity fluctuations enables the determination of the diffusion coefficients of particles, which are converted into a size distribution. The diffusion coefficient is calculated from the time correlation function

$$g(\tau) = A[1 + B \exp(-2Dq^2\tau)] \tag{1}$$

where τ is the sample time, A is the baseline of the correlation function, B is the intercept of the correlation function, $q = [(4\pi n/\lambda_o) \sin(\theta/2)]$ is the scattering vector, n is the refractive index of solution, λ_o is the wavelength of the laser, and θ is the scattering angle.

The time-dependence autocorrelation function of the photocurrent was acquired every 10 s, with 15 acquisitions for each run. The

sample solution was illuminated by a 633 nm laser, and the intensity of light scattered at an angle of 173° was measured by an avalanche photodiode.

The zeta potential in Zetasizer nano ZS was measured using the laser Doppler velocimetry (LDV) technique, (measurement range of 3 nm to 10 μm). In this technique, a voltage was applied across a pair of electrodes placed at both ends of a cell containing the particle dispersion. Charged particles are attracted to the oppositely charged electrode, and their velocity was measured and expressed per unit field strength as the electrophoretic mobility μ_e. Then, the zeta potential was calculated using Henry's equation

$$\zeta = \frac{3\eta}{2\varepsilon F(\kappa a)} \mu_e \tag{2}$$

where ζ is the zeta potential of proteins, μ_e is the electrophoretic mobility, ε is the dielectric constant of water, $F(\kappa a)$ is the function of the dimensionless parameter κa, $\kappa^{-1} = (\varepsilon kT/2e^2I)^{1/2}$ is the double-layer thickness, e is the elementary charge, k is the Boltzmann constant, T is the absolute temperature, $I = 1/2(\sum_i c_i z_i^2)$ is the ionic strength, c_i is the ion concentrations, and a is the characteristic dimension of the protein. Electrophoretic mobility was determined for fixed ionic strength, as regulated by the addition of NaCl of $I = 10^{-3}$, 5×10^{-3}, 10^{-2}, and 0.15 M over the pH range of 2.5 to 10.5.

Viscosity Measurements. The dynamic viscosity of protein solutions was measured using a capillary viscometer equipped with a conductivity sensor of the solution level, according to the procedure described previously in ref 15. The average flow rate of the suspension volume $v_{sus} = 10$ cm³, through a capillary with an internal diameter of R, was calculated to be $\langle V \rangle = v_{sus}/\pi R^2 t$, where t is the time required for the suspension to pass through the capillary. The averaged shear rate $\langle G \rangle = \langle V \rangle/R$ in the capillary was 1.8×10^{-2} s⁻¹. The device was calibrated using a pure liquid of known viscosity, such as water, butyl and amyl alcohol, or ethylene glycol. The precision of the viscosity determination over the range of 1−2 mPa s was estimated to be 0.2%. The concentration of protein solutions used in the viscosity measurements was changed to be within the range of 500−8000 ppm. The intrinsic viscosity was measured for pH values of 5.1, 7.4, and 8.5 and an ionic strength value of $I = 0.15$ M. The density of the protein solutions needed for the viscosity evaluation was determined by a pycnometer.

Results and Discussion

An important parameter characterizing the dynamics of the protein molecules in solution is the diffusion coefficient, which was determined by dynamic light scattering from the autocorrelation function as described above.[16] This method also enables us to determine the hydrodynamic radius of the proteins R_H and its distribution, providing one with information on the polydispersity of the sample. In a preliminary series of experiments, we have determined the dependence of the diffusion coefficient on the concentration of proteins in the bulk, which was varied within the range of 500 to 4000 ppm (5×10^{-4} to 4×10^{-3} weight fraction). Considering that the specific density of both proteins is 1.35 g cm⁻³ (Table 1), this corresponds to the range of the volume fraction of proteins Φ_v of 3.7×10^{-4} to 5.92×10^{-3}. The results obtained for BSA are shown in Figure 1, and those for HSA, in Figure 2. As can be seen, the diffusion coefficient of BSA was practically independent of its bulk concentration, assuming an average value of 6×10^{-7} cm² s⁻¹ for the ionic strength range of 10^{-2} to 0.15 M (pH 6.3).

(15) Adamczyk, Z.; Jachimska, B.; Kolasińska, M. *J. Colloid Interface Sci.* **2004**, *273*, 668.
(16) Berne, J, Pecora, R. *Dynamic Light Scattering with Applications to Chemistry, Biology, and Physics*; Dover Publications: Mineola, NY, 2000.
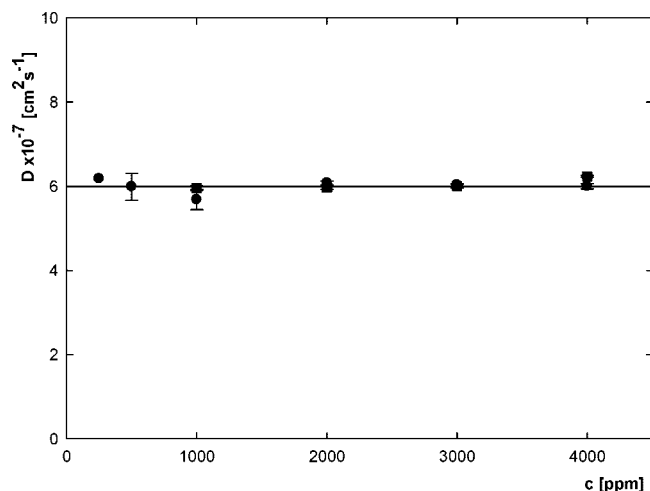
Figure 1. Dependence of the diffusion coefficient of BSA solutions on the bulk concentration c [ppm] determined experimentally for pH 6.3, $T = 298$ K: ■, $I = 1 \times 10^{-2}$ M; ●, $I = 0.15$ M. The line shows the linear fit of the experimental points (i.e., $D = 6 \times 10^{-7}$ cm^2 s^{-1}).
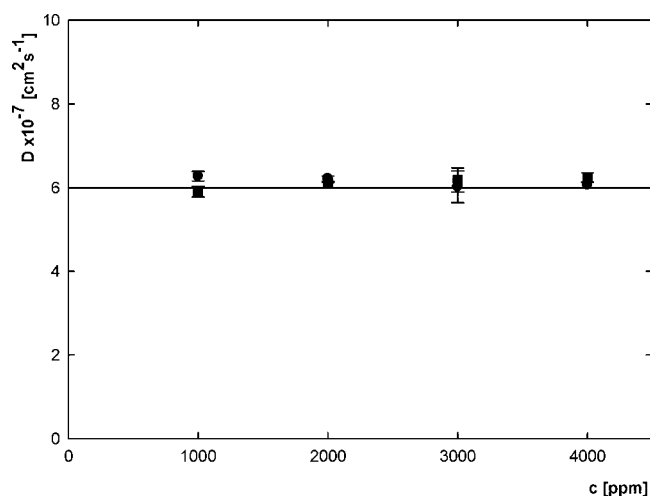
Figure 2. Dependence of the diffusion coefficient of HSA solutions on the bulk concentration c [ppm] determined experimentally for pH 6.3, $T = 298$ K: ■, $I = 1 \times 10^{-2}$ M; ●, $I = 0.15$ M. The line shows the linear fit of the experimental points (i.e., $D = 6.1 \times 10^{-7}$ cm^2 s^{-1}).

It is interesting that similar values of the diffusion coefficient of BSA, which was proven to be independent of pH, were reported by Wang et al.[17] for BSA at ionic strength varying from 10^{-2} to 5 M.

In the case of HSA, similar values, to within experimental error bounds, have been determined in our measurements (Figure 2).

From the diffusion coefficient measurements, one can determine the Stokes hydrodynamic radius of proteins using the known dependence.[6]

$$R_H = \frac{kT}{6\pi\eta D} \qquad (3)$$

Values of R_H calculated from eq 3 using measured diffusion coefficients of BSA are plotted in Figure 3 as a function of pH (for $I = 0.15$ M). As can be seen, R_H calculated by exploiting the entire scattering peak and its maximum value (volume average) are different, although they seem to be pH-independent. Accordingly, the average R_H value for pH 4−9, calculated from the entire peak, was 4.3 nm, and that from the maximum, 3.4 nm (with the ratio of both being 1.26). It is interesting that Park
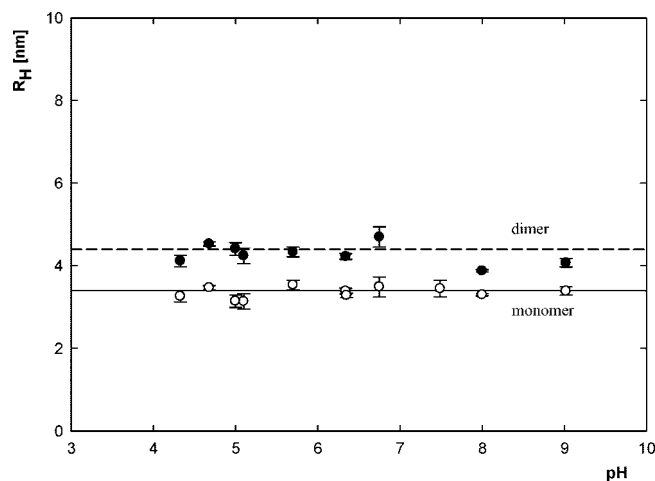
Figure 3. The hydrodynamic diameter R_H of BSA determined by the DLS method, with $c = 1000$ ppm and $I = 0.15$ M. ●, R_H value calculated from the averaged scattering intensity; o, R_H value calculated from the maximum in the scattering peak. The dashed lines denote the limiting analytical solutions calculated from eq 5a for the dimer (upper line) and BSA monomer (lower line).

et al.[18] determined in their measurements similar values of the averaged R_H ($= 3.9$ nm) over the pH range of 5−10. The difference in R_H calculated from the average peak and from the maximum suggests quite unequivocally that BSA and HSA suspensions contained a significant fraction of protein dimers. This is in accordance with previous experimental evidence.[6,10]

A more quantitative analysis of protein aggregation can be performed by considering the shape and dimensions. First, it is instructive to calculate the equivalent sphere radius of BSA, using its molecular volume and density, from the equation

$$v_m = M/\rho_p A_v \qquad (4)$$

where M is the molecular mass of the protein, ρ_p is the protein density, and A_v is Avogadro's number.

Because the known density of both proteins equals 1.35 g cm^{-3}, one can calculate from eq 4 that v_m for BSA and HSA equals 82.5 and 85.0 nm,[3] respectively. Thus, the equivalent sphere radius is $R_s = (3v_m/4\pi)^{1/3}$ (i.e., 2.70 and 2.72 nm for BSA and HSA, respectively).

This simple estimation, compared with the above experimental values of R_H, suggests that the shape of both proteins deviates significantly from a spherical shape. This is in accordance with structural data reported in the protein data bank.[6,10,19] The physical form of the BSA monomer (shown in Table 1) assumes a rather complex cardioidal shape, which, according to Rezwan et al.[6] and others,[9] can be approximated by a prolate spheroid having dimensions of $9 \times 5.5 \times 5.5$ nm^3. Moreover, there are three various domains in the protein structure that are charged differently depending on the pH of the solution.

Using these dimensions, one can calculate the molecular volume of proteins (assuming a prolate spheroid shape) to be $v_s = 4\pi a_s^2 b_s/3 = 142$ nm^3. As can be noticed, this value exceeds 1.73 times previously calculated values of 82.5 and 85.0 nm^3 stemming from the molecular mass. This discrepancy suggests that both molecules form porous structures having a void ratio of $1 - v_n/v_s = 0.42$ for BSA and 0.43 for HSA. Because these values are significantly larger than the usually accepted data for

(17) Wang, L.; Yu, H. *Macrololecules* **1988**, *21*, 3498.
(18) Park, J. M.; Muhoberac, B. B.; Dubin, P. L.; Xia, J. *Macromolecules* **1992**, *25*, 290−295.
(19) RCSB Protein Data Bank, http:// www.pdb.mde-berlin.de.

globular proteins (being close to 0.25^1), this could suggest that the effective dimension of the shorter axis of these proteins is slightly smaller. This hypothesis seems further supported by the fact that in most protein deposition experiments,[3–5] where the thickness of the monolayers is determined, it varied between 3.5 and 5 nm.

In accordance with this observation, the shape of these proteins was approximated in the literature[2] by a prolate spheroid having dimensions of $14.1 \times 3.8 \times 3.8$ nm[3]. Assuming this, one can calculate that $v_s = 4\pi a_s^2 b_s/3 = 106$ nm[3], which exceeds 1.28 times the previously calculated values of 82.5 and 85.0 nm[3] stemming from the molecular mass and gives for the void ratio the value of 0.29. This agrees better with the suggested limit for globular proteins. However, the postulated length of BSA is definitely too large and its thickness is too small in comparison with dimensions acquired from the data bank (Table 1). Therefore, in our further analysis we postulate the "compromise" dimensions of these proteins, which are approximated by a $9.5 \times 5 \times 5$ nm[3] prolate spheroid. In this case, $v_s = 4\pi a_s^2 b_s/3 = 124$ nm[3], which exceeds 1.51 times the molecular volume and gives for the void ratio an acceptable value of 0.33. It is advantageous to approximate the true protein shape by a prolate spheroid shape because its hydrodynamic radius and intrinsic viscosity can be calculated analytically from the hydrodynamic Brenner theory.[20] Using his expression, being the extension of the Stokes−Einstein relationship (eq 3), one can derive for prolate spheroids the analytical expression for R_H

$$R_H = \frac{a_s(\lambda^2 - 1)^{1/2}}{\cosh^{-1}\lambda} \qquad (5a)$$

prolate spheroids, $\lambda = a_s/b_s > 0$

$$R_H = \frac{a_s(1 - \lambda^2)^{1/2}}{\cos^{-1}\lambda} \qquad (5b)$$

oblate spheroids, $\lambda = b_s/a_s < 0$

where b_s and a_s are the shorter and the longer semiaxes of the spheroid, respectively, and λ is the aspect ratio parameter having major significance for predicting the hydrodynamic behavior of spheroidal particles.

It can be calculated from eq 5 that for a prolate spheroid with dimensions of $9.5 \times 5 \times 5$ nm[3], $\lambda = 1.9$ and $R_H = 3.22$ nm. As can be noticed, this theoretical value agrees within experimental error bounds (of about 5%) with $R_H = 3.4$ nm, as determined experimentally from the maximum in the scattering intensity peak.

It is also interesting to calculate the theoretical value of R_H for the dimer of BSA, whose structure is also available from the data bank (Table 1). As can be noticed, the dimer is composed of two BSA molecules attached along their hydrophobic parts as shown in Table 1.[6] The shape of the dimer is rather irregular, having approximate dimensions of $10 \times 9.5 \times 5$ nm[3]. This can be replaced by an oblate spheroid (with the same cross section) having dimensions of $11 \times 11 \times 5$ nm[3]. It can be calculated from eq 5a that for such a prolate spheroid $\lambda = 2.3$ and $R_H = 4.4$ nm. This value is close to the experimental result of 4.3 nm determined using the volume-averaged scattering intensity.

As can be noticed in Figure 4, the pH of BSA solutions did not exert practically any effect on the hydrodynamic radius, which suggests that the degree of aggregation remains practically independent of this parameter.

(20) Brenner, H. *J. Multiphase Flow* **1974**, *1*, 195.
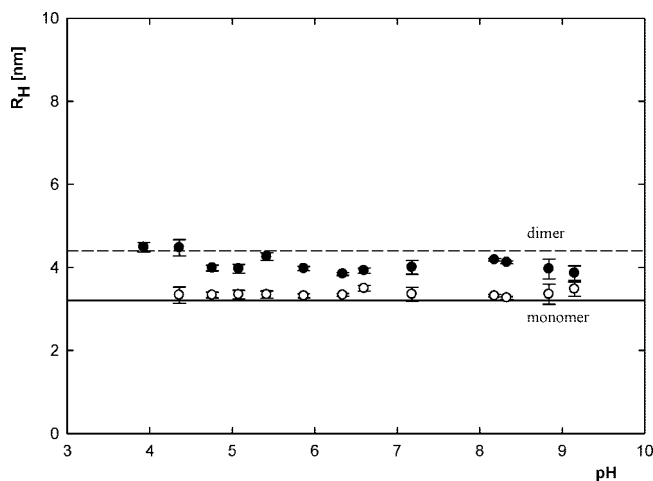
Figure 4. Hydrodynamic diameter R_H of HSA determined by the DLS method with $c = 1000$ ppm and $I = 0.15$ M. ●, R_H value calculated from the averaged scattering intensity; ○, R_H value calculated from the maximum in the scattering peak. The dashed lines denote the limiting analytical solutions calculated from eq 5a for the dimer (upper line) and BSA monomer (lower line).
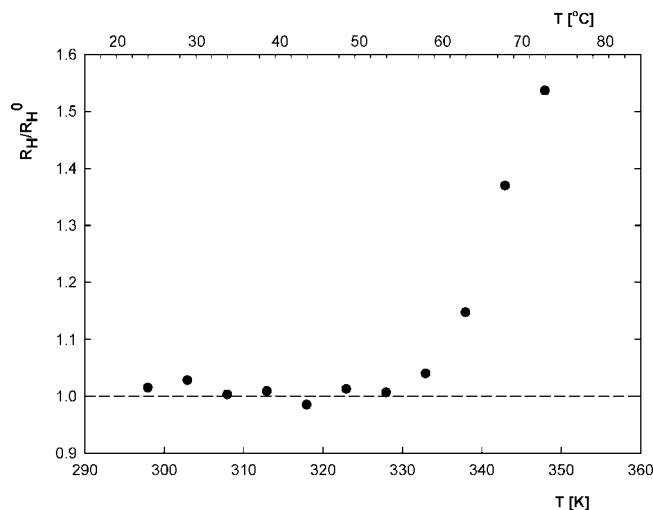
Figure 5. Relative hydrodynamic diameter R_H/R_H^0 (where R_H^0 is the hydrodynamic diameter in $T = 298$ K) of BSA determined by the DLS method as a function of absolute temperature T with $I = 0.15$ M at pH 6.0. The dashed line denotes the initial value.

However, the temperature exerted a pronounced influence on the hydrodynamic radius of BSA, as can be seen in Figure 5 For temperatures higher than 333 K (60 °C), the hydrodynamic diameter of BSA increased significantly, suggesting the appearance of large aggregates, as a result of the denaturation process. The temperature at which denaturation occurs is often referred to as the protein melting point, denoted by T_M. Previous literature data indicate that T_M for BSA is 63 °C,[21] which agrees well with our measurements. Hence, our results indicate that this temperature can be quite easily defined by the DLS techniques.

Other bulk characteristics of protein solutions, which are significant in the interpretation of their adsorption and deposition phenomena, are the effective charge, determined as a function of pH and ionic strength. These data can be directly derived from the electrophoretic mobility measurements, which give the average translation velocity of protein V under a given electric field E. Hence the electrophoretic mobility equals $\mu_e = V/E$. As

(21) Norde, W; Anusiem, A. C. I. *Colloids Surf.* **1992**, *66*, 73–80.

Table 2. Electrophoretic Mobility and the Number of Uncompensated Charges N_c for BSA

$I = 5 \times 10^{-3}$			$I = 1 \times 10^{-2}$			$I = 0.15$		
pH	$\mu_e{}^b$	N_c (e)	pH	μ_e	N_c (e)	pH	μ_e	N_c (e)
3.0	2.2	7.9	3.0	2.1	7.6	3.0	1.4	5.0
4.2	1.52	5.5	4.0	1.8	6.5	4.0	0.97	3.5
5.3	−0.11	−0.4	5.2	−0.07	−0.25	5.2	−0.06	−0.22
6.0	−0.97	−3.5	6.6	−0.85	−3.1	6.6	−0.72	−2.6
7.8	−1.4	−5.0	7.7	−1.4	−5.0	7.0	−0.92	−3.3
8.7	−1.7	−6.1	8.6	−1.7	−6.1	8.6	−1.3	−4.7
9.5	−2.0	−7.2	9.5	−1.9	−6.8	9.6	−1.40	−5.0

Table 3. Electrophoretic Mobility and the Number of Uncompensated Charges N_c for HSA^a

pH	$\mu_e{}^b$	$N_c{}^c$	pH	μ_e	$N_c{}^c$	pH	μ_e	$N_c{}^c$
3.0	2.2	7.9	3.0	1.6	5.8	3.0	1.4	5.0
4.0	1.5	5.4	4.0	1.3	4.7	4.0	0.88	3.2
5.0	−0.09	−0.32	5.0	−0.27	−0.97	5.0	−0.12	−0.03
6.0	−1.3	−4.7	6.0	−1.1	−4.0	6.0	−0.78	−2.8
7.0	−2.2	−7.9	7.0	−1.8	−6.5	7.0	−0.96	−3.5
8.0	−2.2	−7.9	8.0	−1.9	−6.8	8.0	−1.1	−4.0
9.0	−2.1	−7.6	9.0	−2.0	−7.2	9.0	−1.2	−4.3

^{a} HSA, $T = 298$ K, $c = 1000$ ppm, $\eta = 8.9 \times 10^{-3}$ g (cm s)$^{-1}$, $R_H = 3.4 \times 10^{-7}$ cm. ^{b} μm cm V^{-1} s^{-1}. ^{c} $N_c = (6\pi\eta R_H 10^8)/(1.602)\mu_e$.

discussed in ref 22, knowing the electrophoretic mobility enables one to calculate the avarage number of charges per molecule from the Lorenz−Stokes relationship

$$N_c = \frac{6\pi\eta 10^8}{1.602} R_H \mu_e \qquad (6)$$

where μ_e is expressed in μm cm s^{-1} V^{-1} and V is the volt unit.

However, it is worth mentioning that eq 6 becomes less accurate if $\kappa a > 1$, that is, if the thickness of the electric double-layer becomes smaller than the characteristic protein dimension a. It can be estimated that in our case this condition is fulfilled for ionic strength smaller than 10^{-2} M. Nevertheless, even with this limitation, the microelectrophoretic method of determining the uncompensated charge on molecules is much more convenient and reliable than the titration methods,[6] which tends to largely overestimate the charge on molecules. This is so because of the very likely appearance of an ion-exchange process.

The experiemental values of the electrophoretic mobility μ_e and the net number of uncompensated charges per molecule N_c are collected in Table 2. as can be noticed, for pH <5 both proteins acquire positive charge that increases monotonically with decreasing pH. It is interesting that the maximum number of positive charges at pH 3 calculated from eq 6 was rather low, equal to 7.9 for both proteins (at an ionic strength of 5×10^{-3} M). However, for pH >5, the proteins acquire negative charge (−5 elementary charges for BSA and −7.9 for HSA at pH 7 and $I = 5 \times 10^{-3}$ M). It is also interesting that the uncompensated charge determined from the microelectropohoretic measurements is much smaller than that theoretically predicted from the dissociation constant of the amino groups, as calculated by Rezwan et al.,[6] who predicted $N_c = -19.1$ at pH 7 (the ionic strength was unspecified). Hence, the effective charge is only 26−41% of the limiting value predicted from the dissociation equilibrium. This phenomenon observed experimentally for polyelectrolytes[22] is due to the adsorption of counter ions, often referred to as the ion condensation phenomenon. Obviously, the adsorption of counter ions increases with the ionic strength of the supporting electrolyte, which was observed in our case because for $I = 0.15$ M and pH 7 the number of free charges for the BSA molecule was only −3, which amounts to 16% of the overall charge predicted from the dissociation equilibrium. Because these
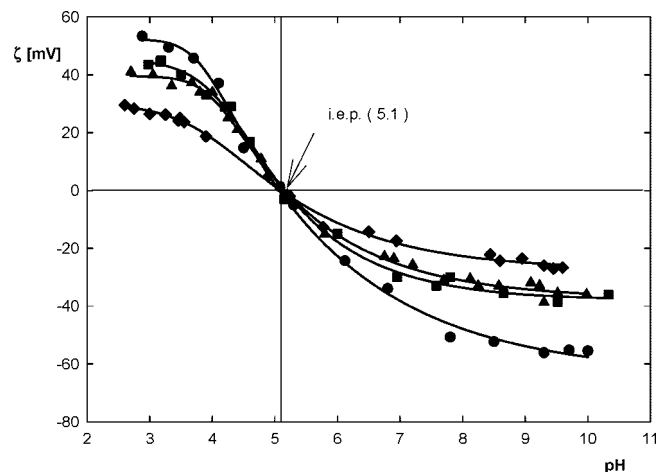
Figure 6. Zeta potential of BSA as a function of pH at $T = 298$ K. The points denote experimental values determined for ●, $I = 1 \times 10^{-3}$ M; ■, $I = 5 \times 10^{-3}$ M; ▲, $I = 1 \times 10^{-2}$ M; and ◆, $I = 0.15$ M.
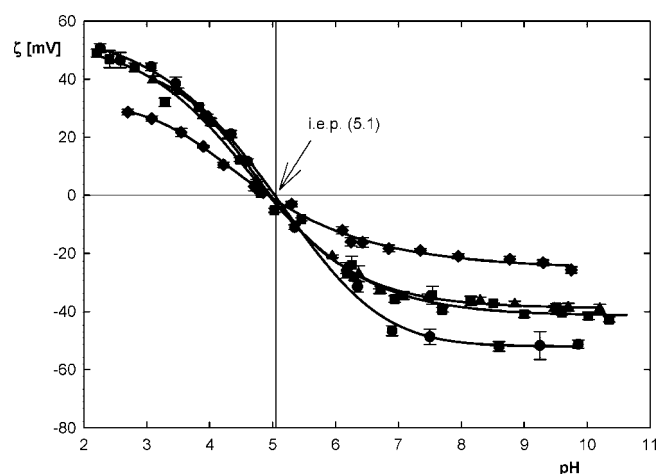
Figure 7. Zeta potential of HSA as a function of pH at $T = 298$ K. The points denote experimental values determined for ●, $I = 1 \times 10^{-3}$ M; ■, 3×10^{-3} M; ▲, $I = 1 \times 10^{-2}$ M; and ◆, $I = 0.15$ M.

values of uncompensated charges are rather small, they probably cannot prevent protein association into dimers as predicted by the hydrodynamic radius measurements.

It is often more convenient to analyze the electrokinetic behavior of proteins in terms of zeta potential ζ, which is commonly used in the interpretation of colloid, polyelectrolyte, and protein suspension stability.[23] The zeta potential is connected with the measured electrophoretic mobility via the constituent dependence (eq 2).

The dependence of the zeta potential on pH is shown in Figure 6–8. As can be seen in Figure 5, the zeta potential of BSA decreased from 50 mV at pH 3 to −55 mV at pH 10 for $I = 1 \times 10^{-3}$ M. For higher ionic strength of $I = 0.15$, the zeta potential was 30 mV at pH 3 and −30 at pH 10. Independently of the ionic strength, however, a zero value of the zeta potential was attained for pH 5.1, which is usually referred to as the izoelectric point (iep). The same iep was also determined for HSA (Figure 7). It is interesting that the iep's for BSA and HSA found in our work agree with the data reported in the literature, which were found

(22) Adamczyk, Z.; Bratek, A.; Jachimska, B.; Jasiński, T.; Warszyński, P. *J. Phys. Chem. B* **2006**, *110*, 22426–22435.

(23) Adamczyk, Z. *Adv. Colloid Interface Sci.* **2006**, *100–102*, 267–347.
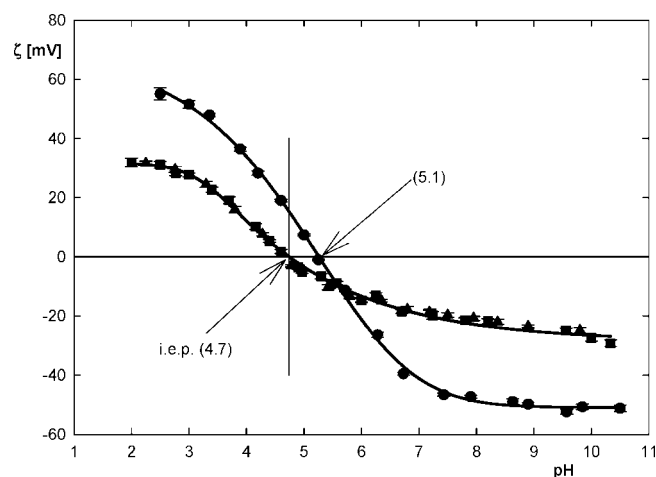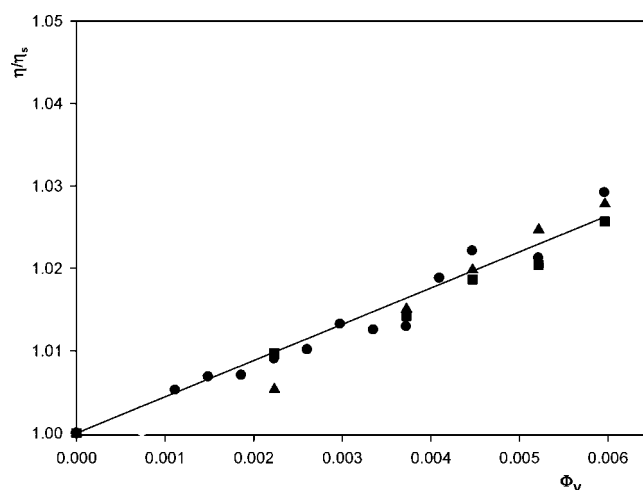
Figure 8. Zeta potential of BSA as a function of pH determined at $T = 298$ K for various solutions: the points denote experimental values determined for ◆, 1×10^{-2} M MES + 0.15 M NaCl; ▲, 1×10^{-2} M MES-TRIS + 0.15 M NaCl; and ●, 1×10^{-3} M MES.

to be 4.7−5.1 for BSA[6,7] and 4.7−4.9 for HSA.[24,25] The small deviations can be explained by the use of various buffers used to prepare protein solutions used in these experiments. As can be seen in Figure 8, for example, the iep of BSA is decreased from pH 5.1 in the MES buffer to pH 4.7 when the MES-TRIS buffer is used.

Our experimental iep data can be compared with theoretical predictions taking into account the amino acid composition of these proteins and the pK values of the side chains.[6,7,26,27] These parameters are present in Table 4. Then, by summing up contributions stemming from various amino acids as a function of pH, it becomes possible to calculate the theoretical charge and iep of the protein. This simple approach assumes that all ionizable amino acid groups are accessible to water. In our calculations, the pK values were taken from the literature, and the amino acid sequence for BSA was taken from Hirayama et al.[28] and the protein data bank.[19] From these theoretical calculations, the iep of BSA was predicted to be 5.5. Our experimental result of 5.1 is slightly smaller than the theoretical estimation, which can be explained by the fact that a small part of the charged amino acids is not accessible to water.

As suggested by previous measurements for particles[15] and polyelectrolytes,[22] additional information on the shape of particles forming suspensions and their degree of aggregation can be extracted from dynamic viscosity measurements carried out for a low range of volume fractions. The slope of the relative viscosity of a suspension η/η_s (where η is the suspension viscosity and η_s is the solvent viscosity) with respect to its volume fraction Φ_V, called the intrinsic viscosity, can be quantitatively related to the shapes of molecules or aggregates.

Such results obtained for BSA are presented in Figure 9, where the dependence of the relative viscosity of the BSA solutions protein η/η_s on $\Phi_V < 0.008$ and $I = 0.15$ M is shown. As can be seen, results obtained for the pH range of 4−9 could be well

(24) Abramson, H. A., Gorin, M. L. S. *Electrophoresis of Proteins*; Hafner Publishing Company, New York, 1942.

(25) Dawson, R. M. *Data for Biochemical Reaserch*; Clarendon Press: Oxford, U.K., 1986.

(26) Burton, W. G.; Nugent, K. D.; Slattery, T. K.; Summers, B. R.; Snyder, L. R. *Chromatogr. A* **1988**, *443*, 363−379.

(27) Berg, J. M.; Tymoczko, J. L.; Stryer, L. *Biochemistry*, 5th ed; W. H. Freeman: New York, 2002.

(28) Hirayama, K.; Akashi, S.; Furuya, M.; Fukuhara, K *Biochem. Biophys. Res. Commun.* **1990**, *173*, 639−646.

Figure 9. Dependence of the relative viscosity of BSA solutions η/η_s on the volume fraction Φ_V determined for $T = 298$ K, $I = 0.15$ M, and various pH values. The solid line denotes linear fits with a slope equal to 4.5. The points denote experimental data obtained for ●, pH 7.4; ■, pH 5.1; and ▲, pH 8.5.

Table 4. Amino Acid Composition of BSA and pK Values.

amino acid	BSA	charge	pK
Arg	23	+	12.5
His	17	+	6.0
Lys	59	+	10.8
Asp,Glu	100	−	4.1
Tyr	19	−	10.9
Cys	35	−	8.3
iep	5.51		

reflected by the linear dependence of the slope (intrinsic viscosity), which is equal to 4.5.

It is interesting to compare this result with theoretical predictions stemming from hydrodynamic theories of dilute suspension viscosity. As is well known, for rigid, spherical particles, the Einstein model predicts that the intrinsic viscosity $[\eta] = 2.5$. This theory has been generalized by Brenner,[20] who considered the case of spheroidal particles immersed in linear velocity fields. In the case of prolate or oblate spheroids in a simple shear flow (pertinent to our measurements), the intrinsic viscosity of their suspensions can be evaluated from the analytical dependence

$$[\eta] = 5Q_1(\lambda) - Q_2(\lambda) + 2Q_3(\lambda) \tag{7}$$

where Q_1, Q_2, and Q_3 are functions of the aspect ratio λ parameter given explicitly in refs 20 and 22.

Assuming as before that BSA has a prolate spheroid shape with dimensions of $9.5 \times 5 \times 5$ nm^3 ($\lambda = 1.9$), one can predict from eq 7 that the theoretical value of the intrinsic viscosity, corrected for the effective volume, equals 4.4. For the compact dimer having the shape of an oblate spheroid with dimensions of $11 \times 11 \times 5$ nm^3, the theoretical value of the intrinsic viscosity equals 4.5. As can be noticed, the average value of the monomer and the compact dimer is very close to the experimentally measured value for the entire pH range studied.

It is also interesting that for higher-rank aggregates the intrinsic viscosity values predicted from eq 7 are much higher, for example, 9.7 (for a linear aggregate formed from three BSA molecules) and 13.8 for a four-molecule aggregate. Hence, the dynamic viscosity measurements confirmed the association of BSA into a compact dimer structure, and excluded the possibility of forming higher-order structures.

Conclusions

Measurements of the diffusion coefficients of BSA and HSA (hydrodynamic radii) suggested that the shape of these molecules in a monomeric state can be approximated by prolate spheroids having dimensions of $9.5 \times 5 \times 5$ nm^3. However, these experimental data also suggested that there can be an appreciable number of compact dimers whose shape was approximated by an oblate spheroid having dimensions of $11 \times 11 \times 5$ nm^3.

Further characteristics of proteins in solutions have been acquired from the electrophoretic measurements carried out as a function of pH and ionic strength. This enabled one to determine in a simple and direct way the number of uncompensated (electrokinetic) charges on protein molecules under various ionic conditions, which was found to be considerably smaller than the theoretical charge predicted from dissociation equilibria. It was also revealed experimentally that the isoelectric point of both proteins was located at pH 5.1.

The hypothesis of protein association into dimers was further supported by dynamic viscosity measurements of protein solutions. Simultaneously, these measurements excluded the possibility of forming linear aggregates of higher rank.

Therefore, it was concluded that the combination of dynamic viscosity and dynamic light scattering can be exploited as a convenient tool for determining and detecting not only the onset of protein aggregation in suspensions but also the form and composition of these aggregates.